Review

J. Mex. Chem. Soc. **2024**, *68*(4)
Special Issue

ISSN-e 2594-0317

A Review of Mexican Contributions to Li_2CuO_2 and its Chemical Modifications as Cathode Materials for Lithium-Ion Batteries

B. A. García-Carrillo[1], A de J Martínez[1], E. L. Jiménez-Cabañas[2], MA Martínez Cruz[*,3,4], C. Juarez-Yescas[*,5,6], G. Ramos-Sánchez[*,2,7]

[1]Departamento de Química, Universidad Autónoma Metropolitana – Iztapalapa, Av. San Rafael Atlixco, Leyes de Reforma 1ra secc, Iztapalapa 09340 CDMX, México.
[2]Departamento de IPH, Universidad Autónoma Metropolitana – Iztapalapa, Av. San Rafael Atlixco, Leyes de Reforma 1ra secc, Iztapalapa 09340 CDMX, México.
[3]Instituto de Investigación en Materiales, Universidad Nacional Autónoma de México, Cd. Universitaria, Del. Coyoacan, CP 04510, CDMX México.
[4]Centre for Cooperative Research on Alternative Energies (CIC energiGUNE), Basque Research and Technology Alliance (BRTA), Technology Park, Albert Einstein 48, Vitoria-Gasteiz, Avala 01510, Spain.
[5]Department of Chemistry, University of Illinois Urbana−Champaign, Urbana, Illinois 61801, United States
[6]Materials Research Laboratory, University of Illinois Urbana−Champaign, Urbana, Illinois 61801, United States.
[7]Laboratorio Nacional Conahcyt de Baterías Ion-Li y Post Li para el diseño y escalamiento de materiales y dispositivos (LNC-BIL-DEMo).

***Corresponding author:** MA Martínez Cruz, email: miguee.cm@gmail.com; C. Juarez-Yescas, email: carlosj3@illinois.edu; G. Ramos-Sánchez, email: gramos@xanum.uam.mx

Received May 25th, 2024; Accepted August 2nd, 2024.

DOI: http://dx.doi.org/10.29356/jmcs.v68i4.2294

Abstract. Over the past few decades, battery research has primarily focused on reducing costs and increasing energy density. There have been significant efforts to identify alternative cathode materials that could replace cobalt-based ones, with the goal of finding more environmentally friendly and cost-effective options. In this context, copper-based cathodes have emerged as promising candidates. The appeal of copper-based cathodes lies in their relatively high abundance, particularly in Mexico, their high theoretical energy density, and the potential to enhance their properties by altering their chemical structure. In recent years, numerous research initiatives in Mexico have aimed to make Li_2CuO_2 cathodes a viable option. This review examines the recent advances and future perspectives of these efforts, with a particular emphasis on the latest attempts to modify the synthesis route and incorporate multiple dopants to create synergistic effects.
Keywords: Li_2CuO_2; cation doping; anion doping; dual doping; in situ analyses.

Resumen. Durante las últimas décadas, la investigación sobre baterías se ha enfocado principalmente en la disminución de costos y el incremento de la densidad energética. Se han realizado importantes esfuerzos para identificar materiales catódicos alternativos que podrían reemplazar a los materiales basados en cobalto, con el objetivo de encontrar opciones rentables y con menor impacto al medio ambiente. En este contexto, los materiales catódicos basados en cobre se han convertido en candidatos prometedores. El interés por los cátodos basados en cobre radica en su abundancia relativamente alta, particularmente en México, su alta densidad energética teórica y la cualidad de mejorar sus propiedades alterando su estructura química. En los últimos años, numerosas propuestas de investigación en México han tenido como objetivo hacer de los cátodos de Li_2CuO_2 una opción viable. Este resumen recopila los avances recientes y las perspectivas a futuro de estos esfuerzos,

J. Mex. Chem. Soc. **2024**, *68*(4)
Special Issue

ISSN-e 2594-0317

con especial énfasis en los últimos intentos de modificar la ruta de síntesis y, a su vez, incorporar múltiples dopantes para crear efectos sinérgicos.
Palabras clave: Li_2CuO_2, dopaje catiónico, dopaje aniónico, dopaje dual, análisis in situ.

Introduction

In recent years, concerns about climate change and greenhouse gas (GHG) emissions have grown significantly. The impact of GHG on humanity's immediate future is uncertain; however, most environmental forecast studies suggest a challenging future if emissions continue to rise. To mitigate GHG emissions, a shift towards a more renewable energy sector appears to be the most direct approach. Several milestones have been achieved in this regard over the past few years. The installation of solar power reached 1185 GW in 2022 [1], wind power reached 906 GW in 2021 [2] and tidal power generation reached 527 MW [3] worldwide. These efforts underscore the significance of the energy transition and the commitment of some sectors to enhance the utilization of renewable energy. However, as the utilization of renewable energy increases, so does the need for energy storage solutions. Energy storage is the ideal solution to synchronize energy production and consumption for the benefit of the consumer, who would otherwise need to adjust to periods of peak production.

Storing energy in batteries in the form of chemical energy has advantages in terms of energy density, voltage and response time when compared to mechanical energy storage systems. However, for large scale renewable energy storage, improvements still need to be made. One of the significant challenges lies in the cost associated with energy storage. Lithium-ion batteries (LIB) require costly production processes, demanding substantial amounts of transition metals and lithium to produce cathode materials. In this regard, Mexican institutions have set to replace cobalt chemistries for more abundant elements like copper. In addition, Mexico's legislation has stablished lithium sources as a strategic mineral. This has led to the creation of LitioMx, a state-owned company, to develop the extraction and production of lithium products [4]. This development and Mexico's signing of the Paris agreement in 2016 creates a scenario where the promise of LIBs holds a bright future and a strong commitment to reduce GHG emissions.

Copper-lithium oxides have been reported since early 70's, where the specific crystalline structure seems suitable for several magnetic and electric applications [5–7]. Copper in an +2 oxidation state forms crystalline structures consisting of edge-sharing $[CuO_4]$ nearly square planar units lying on the bc plane which are linked together along the b-axis. Joining the chains between them are [LiO] layers in which the local symmetry around the metallic atoms is D2d [7]. The nature of the structure with two lithium ions per copper make it theoretically possible to achieve a specific capacity of 490 $mAhg^{-1}$. However, while the oxidation of Cu^{+2} to Cu^{+3} does take place during charging, any additional capacity has been demonstrated to arise from irreversible oxygen evolution [8–12]. Seminal works have focused on deciphering the changes occurring during lithiation, indicating that irreversible phase transformations cause poor long-term cycling. The transition from Li_2CuO_2 to $Li_{1.5}CuO_2$ seems to be the more stable transformation, yielding in only one quarter of the full theoretical capacity. Further works have relied on doping and the formation of solid solutions with other metal ions to increase the stability and specific capacity [10,11,13]. However, the exact nature of doping and its effect remained elusive. Perea-Ramírez et al. [14] conducted a study on the electronic structure of Li_2CuO_2 when doped with various transition metals. The impact of these transition metals on the density of states is significant, as they shift the preference from oxygen states to metallic ones. This shift potentially increases the useable capacity before reaching oxygen evolution potentials. Furthermore, the study demonstrated that there are several strategies available to modify the electronic structure, making the use of Li_2CuO_2 in LIBs feasible [14].

This review begins by examining the properties of unmodified Li_2CuO_2. It then dives into the effects of doping with a single transition metal, such as Ni, Co, Fe, and Mn, which were explored as potential dopants to enhance stability. Subsequently, the use of anionic dopants and in situ XRD techniques are also summarized. The formation of mixed phases is subsequently reviewed, followed by an evaluation of the effects of multiple doping. The review presents information from the past eight years to assess the potential of copper as a base metal for commercial Lithium-Ion Battery (LIB) applications.

J. Mex. Chem. Soc. **2024**, *68*(4)
Special Issue

ISSN-e 2594-0317

Properties of unmodified Li_2CuO_2

Generally, Li_2CuO_2 is synthesized using a conventional solid-state synthesis method, using lithium oxide and copper oxide as the precursors (eq. 1), with an excess of lithium oxide to compensate for loss of lithium as a result of sublimation. This reaction is carried out at 800 °C, common factors affecting yield are temperature, heating, and cooling ramps as well as temperature hold times.

$$CuO + Li_2O \rightarrow Li_2CuO_2 \qquad \text{eq. 1}$$

To modify the material, reaction 1 can be modified to include other precursors in the appropriate stoichiometric ratios to form the desired compound. For instance, NiO has been used to integrate Ni to form solid solutions, similarly CuF_2 has been added to add fluorine as an anodic dopant [15]. The quantities of these extra compounds should be carefully examined since sufficiently high amounts can lead to the formation of secondary phases. Moreover, since the oxidation state of copper in CuO is 2+, the addition of other compounds with different oxidation states should be carefully chosen to compensate the charges.

Li_2CuO_2, upon exposure to atmospheric conditions, it decomposes to oxides, including CuO, Cu_2O and Li_2O, as well as the possible generation of Li_2CO_3 ($Li_2CuO_2 + CO_2 \rightarrow Li_2CO_3 + CuO$). These degradation mechanisms consequently decrease battery capacity. For this reason, samples must be stored under inert gas to prevent the formation of segregated phases or surface modifications.

In a battery, the electrochemical reactions that Li_2CuO_2 undergoes are as follows:

$$Li_2CuO_2 \rightarrow Li_{1.5}CuO_2 + 0.5\ Li^+ + 0.5\ e^- \qquad \text{eq. 2}$$

$$Li_{1.5}CuO_2 \rightarrow LiCuO_2 + 0.5\ Li^+ + 0.5\ e^- \qquad \text{eq. 3}$$

$$LiCuO_2 \rightarrow CuO + 0.5\ O_2 + Li^+ + e^- \qquad \text{eq. 4}$$

In Fig. 1, the charge/discharge profiles for Li_2CuO_2 at two potential windows are shown (C/15), the corresponding 50th cycles are shown as dashed lines [16]. For the first potential window of 1.5 to 4.2 V, the specific capacity is approximately 225 mAhg^{-1}, and the discharge capacity is 180 mAhg^{-1}. However, during the second cycle, the discharge capacity begins to decrease continuously, which is attributed to the irreversible changes in Li_2CuO_2, impeding the intercalation of Li^+ ions. For the profile at the potential window of 2.1 to 3.8 V, during the first cycle, a charge capacity of 160 mAhg^{-1} and a discharge capacity of 110 mAhg^{-1} is observed. Starting from the second cycle, the behavior is stabilized due to the extraction of one lithium ion from Li_2CuO_2, indicating improved structural stability.

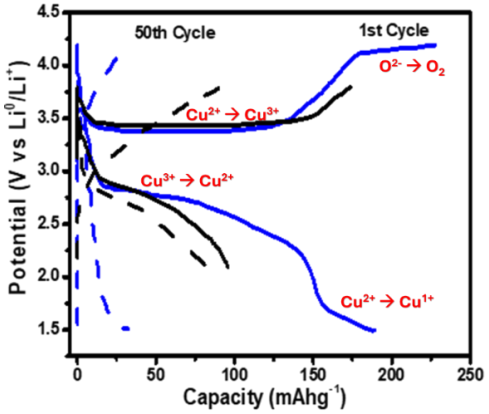

Fig. 1. Galvanostatic charge/discharge characteristics on the first 50 cycles with Li_2CuO_2 cathodes in extended voltage range from 1.5 - 4.2 V (blue) and shortened voltage window from 2.1 - 3.8 V (black). Reprinted from data in [16] with the authors permission.

J. Mex. Chem. Soc. **2024**, *68*(4)
Special Issue

ISSN-e 2594-0317

Structural phase transition and O_2 evolution processes occur during the delithiation of various cathode materials such as layered oxides, Li_2CuO_2, being not the exception. Perea-Ramirez et al. performed electronic structure calculations of pristine Li_2CuO_2 and modified with other transition metal ions, which demonstrated that the evolution of oxygen at potentials higher than 3.8 V was due to a greater density of states of oxygen close to the Fermi level with respect to Cu, promoting its oxidation and, as consequence the formation of phases that inhibit structural reversibility and affect the electrochemical performance of Li_2CuO_2 [14]. This situation generates the need to propose alternatives to improve its structural and electrochemical behavior.

Effect on properties of Li_2CuO_2 doped with metallic cations

By incorporating metal cations from other transition metals (TM) into Li_2CuO_2, we can enhance its reversible capacity and stability. This provides a clear alternative for mitigating the drawbacks of the unmodified Li_2CuO_2. However, depending on the specific nature of the dopant, we can find several outcomes.

Fig. 2 provides a summary of the characterization of Li_2CuO_2 in its unmodified form, as well as its modifications when combined with Mn, Fe, or Ni. The materials were synthesized via the solid-state method and also characterized using EPR, Mossbauer, and XRD techniques [12]. This characterization demonstrates the effective incorporation of TMs into Li_2CuO_2, forming a solid solution without the presence of a secondary phase. ^{7}Li MAS NMR spectra of Li_2CuO_2 and TMs-Li_2CuO_2 are shown in Fig. 2**(a)**. The spectra exhibit two signals, one at near 0 ppm and the other at 340 ppm. The signal near 0 ppm is attributed to surface impurities such as LiOH or Li_2CO_3, which are not detectable by XRD. The signal at 340 ppm arises from Fermi contact associated with interchain interaction via Cu-O-Ti-O-TMs, where spin transfer occurs from paramagnetic copper to lithium through oxygen [19]. The slight shifts in the signals indicate changes in the local chemical environment of lithium due to the presence of TMs.

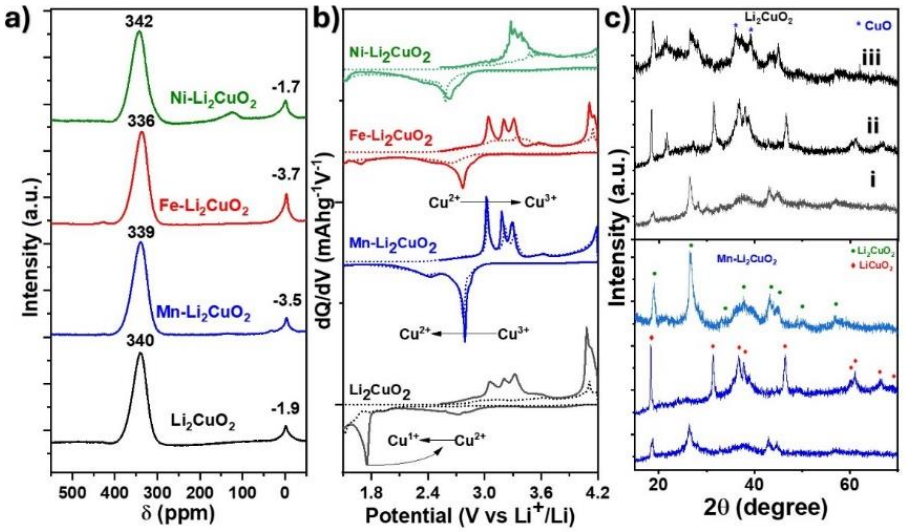

Fig. 2. (a) ^{7}Li MAS NMR spectra and **(b)** dQ/dV of Li_2CuO_2 and MTs-Li_2CuO_2, and **(c)** ex situ XRD patterns of Li_2CuO_2 and Mn-Li_2CuO_2. XRD patterns of both samples correspond to: i) discharge of the first cycle, ii) charge of the second cycle, and iii) discharge of the fifth cycle. Figure reproduced from [12] with the author's permission.

The electrochemical performance of the materials was analyzed within a potential window of 1.5 to 4.2 V vs Li^+/Li. dQ/dV profiles for the second and fifth cycles of each material are presented In Fig. 2**(b)**.

J. Mex. Chem. Soc. **2024**, *68*(4)
Special Issue

ISSN-e 2594-0317

Li_2CuO_2 and Mn- and Fe-Li_2CuO_2 exhibit three oxidation peaks between 2.8 – 3.3 V and one reduction peak (or two in Mn-Li_2CuO_2 case) between 3.0 – 2.4 V in the second cycle. These peaks are associated with different lithiation states, as reported by Masquelier et al. [8]. However, at around 3.9 V, another oxidation peak associated with the oxidation of O^{2-} to O_2 is observed, which is more intense for Li_2CuO_2 and Fe-Li_2CuO_2, indicating a greater O_2 evolution. O^{2-} vacancies are probably generated it the lattice inducing structural instability, forming CuO, which is reduced at 1.8 V, which was observed in both materials. For material modified with Mn, the reduction peak does not occur, indicating lowered O^{2-} oxidation. On the other hand, in the material modified with Ni, oxidation processes occur at a different potential than the pristine material. This is likely due to the oxidation of Ni^{2+} to Ni^{3+}, causing nickel to leave the lattice, and forming a new phase like $LiNiO_2$ [9].

Mn-Li_2CuO_2 shows no significant changes between the second and fifth cycles. The presence of manganese in the lattice enhances the structural reversibility of Li_2CuO_2, which was confirmed by conducting ex situ XRD analysis at different charge and discharge cycles (Fig. 2**(c)**). This analysis confirmed the presence of orthorhombic and monoclinic phases during lithium-ion insertion and extraction respectively, which is not observed for pristine Li_2CuO_2.

Based on these results, it is clear that transition metals as dopants, improve the electrochemical performance, such as increasing specific capacity or enhancing material structural stability. For example, Fe or Ni might serve as active cations during oxidation, providing greater capacity, while Mn doping is inactive but can serve as a structural pillaring agent.

Considering these results, Li_2CuO_2 has been simultaneously doped with Mn^{4+} and Co^{2+} or Ni^{2+} ions to improve its structural stability and increase its capacity and retention [20]. The doping was carried out using a molar concentration of 2.5 % of each TM through solid state synthesis in which a ball milling process was used for 10 minutes at a frequency of 25Hz.

The XRD patterns of the samples Co-Li_2CuO_2, Ni-Li_2CuO_2, CoMn-Li_2CuO_2 and NiMn-Li_2CuO_2 (as shown in Fig. 3) confirm that all samples share the same structure. They all possess the orthorhombic phase characteristic of Li_2CuO_2, without any formation of segregated phases. These results corroborate the formation of a pure phase even with the doping of two TMs, implying that all the dopant ions can be incorporated into the structure of the pristine material and are coordinated in a square plane coordination. The specific case for Co^{2+} ions is interesting since the normal coordination in this geometry is complicated, so the distortion of the unit cell that may be generated is imperceptible at these conditions.

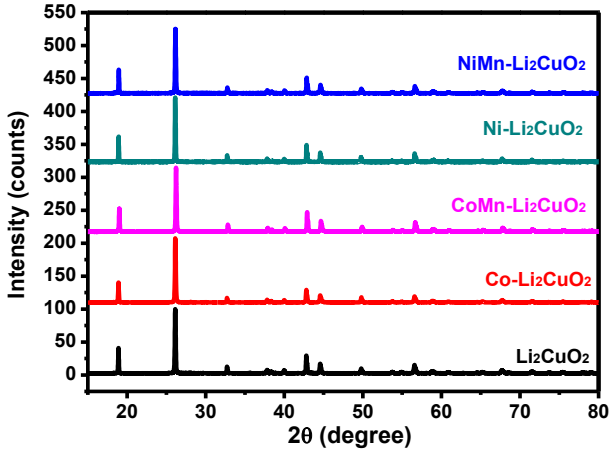

Fig. 3. XRD pattern of the Li_2CuO_2 and all modifications with one or two transition metal ions. Figure reproduced from [20] with the author's permission.

Regarding the electrochemical behavior, the charge-discharge profiles allow us to identify that Li_2CuO_2 synthesized with this methodology increases its capacity and allows it to retain more than 50% of the

J. Mex. Chem. Soc. **2024**, *68*(4)
Special Issue

ISSN-e 2594-0317

capacity after 50-cycles (Fig. 4 **(a)**). In the samples doped with two types of cations (labeled as CoMn-Li_2CuO_2 and NiMn-Li_2CuO_2), it is clear that they do not yield higher capacity than the pristine material (Fig. 4 **(b)**). The material doped with Co^{2+} cations (labeled as Co-Li_2CuO_2) has slightly better electrochemical behavior than Li_2CuO_2 because it maintains marginally greater retention (Fig. 4 **(c)**). Many reports recently have included more than one dopant in the structure, claiming improved properties [21–23], based on results herein mentioned, dual doping has a net positive effect, although just marginal.

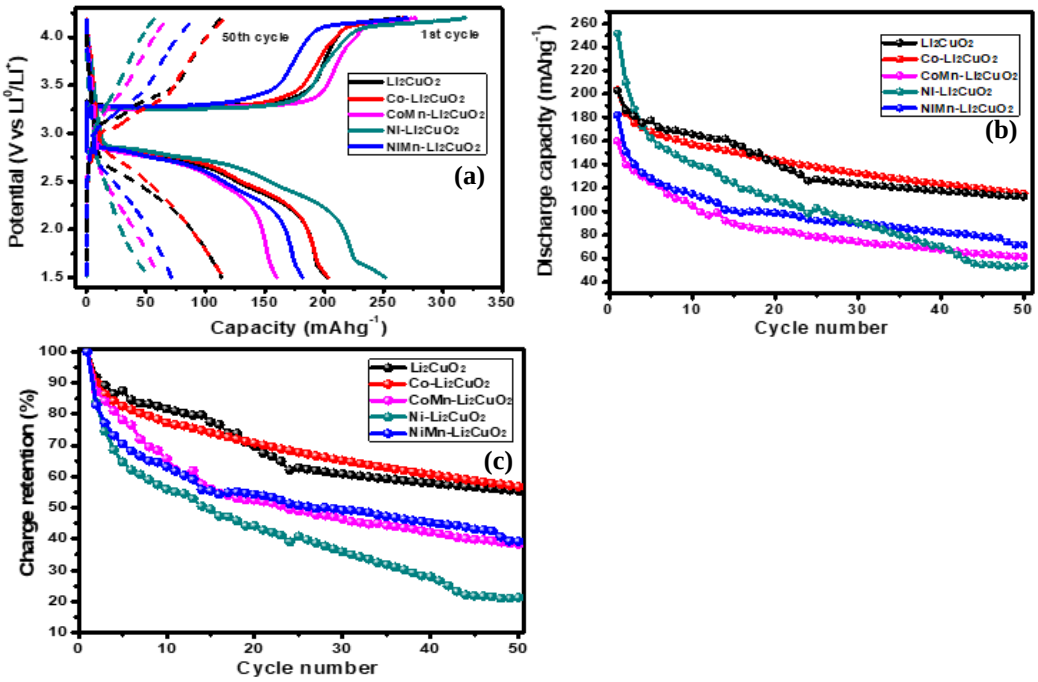

Fig. 4. (a) Galvanostatic charge/discharge profiles on the first and fiftieth cycles with Li_2CuO_2 and doped samples in extended voltage window 1.5-4.2 V, **(b)** Cyclic performance and **(c)** Charge retention during discharge. The Li^0|1 M $LiPF_6$|Active material: carbon black: PVDF (75:15:10 wt%) cell was cycled at C/10 at 25°C. Figure reproduced from [20] with the author's permission.

Fluorine as an anionic doping agent

Anion doping Li metal oxide cathode materials has been reported as an alternative to increase the electrochemical performance, voltage stability and potentially inhibiting the evolution of oxygen [24–26]. As pointed out in previous sections, the predominant failure mechanism for Li_2CuO_2 is the evolution of O_2 during charging as cycling progress, limiting its practical application despite its promising characteristics. A lot of efforts have been made to incorporate fluorine into the structure of Li_2CuO_2 via a simple modified solid-state reaction [15]. Given differences in valence between O and F, it was expected that the doped Li_2CuO_2 would yield a Cu and O deficient structure, as suggested by equation 5. Different compositions of the F-doped Li_2CuO_2 were explored (2.5, 5.0 and 10 mol%). XRD analysis showed that the cell parameters in the a and c directions decreased as a function of fluorine concentration [15]. The decrease in cell parameters has been attributed to the smaller ionic radius of F (1.36 Å) occupying oxygen sites (O ionic radius: 1.40 Å); specifically, in planes 200 and 013.

$$Li_2O + (1-2x)CuO + xCuF_2 \rightarrow Li_2Cu_{1-x}O_{2-2x}F_{2x} \qquad \text{Eq. 5}$$

J. Mex. Chem. Soc. **2024**, *68*(4)
Special Issue

ISSN-e 2594-0317

Cycling the F-doped materials under constant current (0.1 C), showed the positive effects of the introduction of fluorine. The unmodified material exhibited a characteristic poorly defined plateau during the first charge, and a low initial Coulombic efficiency (55 %). In contrast, F-doped materials showed a well-defined plateau near 3.3 V, with improvement in Coulombic efficiency, up to 69 % (Fig. 5**(A)**). While all the F-doped samples showed higher overpotential during initial charge, the 2.5 % and 5.0 % showed less overpotential and improved reversibility. Among the F-doped variants, 5.0 mol% F-doping yielded the best electrochemical performance. Although the capacity retention at cycle 10 was only 57 % of the initial capacity, Coulombic efficiency improved to 99 % (Fig. 5**(B)**). Overall, the F-doped cuprate (5.0 mol%) demonstrated improved capacity retention, discharging 133 $mAhg^{-1}$ compared to 83 $mAhg^{-1}$ for the pristine Li_2CuO_2 on the 10^{th} cycle. Performance gains were not observed when F-doping exceeded 5.0 mol %. XRD refinement revealed that the introduction of the fluorine precursor during the synthesis of F-doped Li_2CuO_2 promoted the formation of a secondary CuO phase [15]. As a result, any doping beyond the 5.0% threshold proved to be counterproductive.

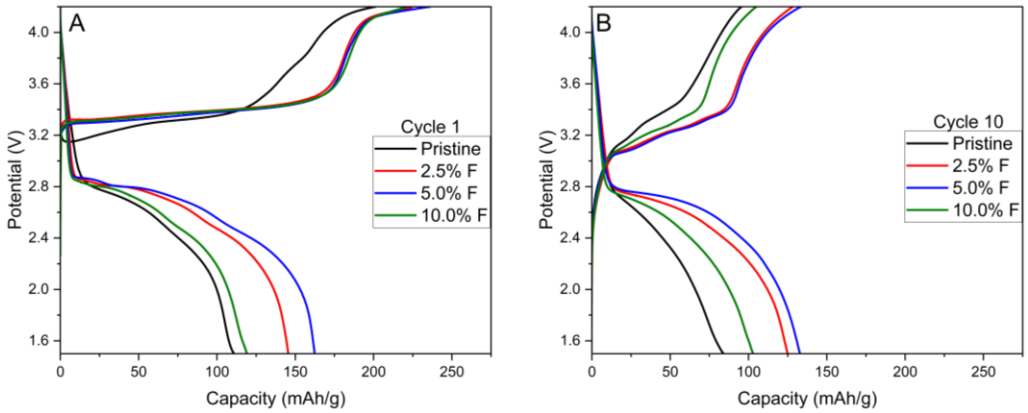

Fig. 5. Typical voltage profiles of Li^0|1 M $LiPF_6$|Active material: carbon black: PVDF (75:15:10 wt %) at first **(A)** and tenth **(B)** cycle. Cycling rate: 0.1C. Adapted with permission from Ref.[15]. Copyright 2020 American Chemical Society.

In-Situ XRD and gases generation during cycling

In situ techniques are needed to gain direct information about chemical reactions and transformations beyond that obtained by the current-voltage curves. In this section gas detection and structural transformations are revised.

To assess the effectiveness of inhibiting O_2 evolution, Differential Electrochemical Mass Spectrometry (DEMS) was employed during a voltage scan in the positive direction. The scan ranged from the open circuit potential up to 4.5 V vs Li, ensuring O_2 evolution. Both pristine Li_2CuO_2 and 5.0 mol% F-doped Li_2CuO_2 were studied. For the pristine Li_2CuO_2, results confirmed the O_2 formation starting at 4.1 V (Fig. 6). The correlation between ionic current and faradaic current associated to O_2 evolution was the first reported for Li_2CuO_2, confirming that the second oxidation process at 4.35 V is the lattice O oxidation. Approximately 23.3 % of oxygen in the cathode was lost as O_2 (0.032 mmol) during the electrochemical perturbation. Notably, the presence of fluorine improved electrochemical performance by inhibiting oxygen evolution across all explored potentials. The voltammogram for the doped material still exhibited an oxidation peak related to oxygen, but without actual oxygen evolution. This behavior could be attributed to the reversible oxygen redox reactions as previously reported [27]. Nonetheless, F-doped Li_2CuO_2 still suffers from significant capacity fade, however these incremental improvements suggest that leveraging novel modification methods can be used to further improve the material's properties.

J. Mex. Chem. Soc. **2024**, *68*(4)
Special Issue

ISSN-e 2594-0317

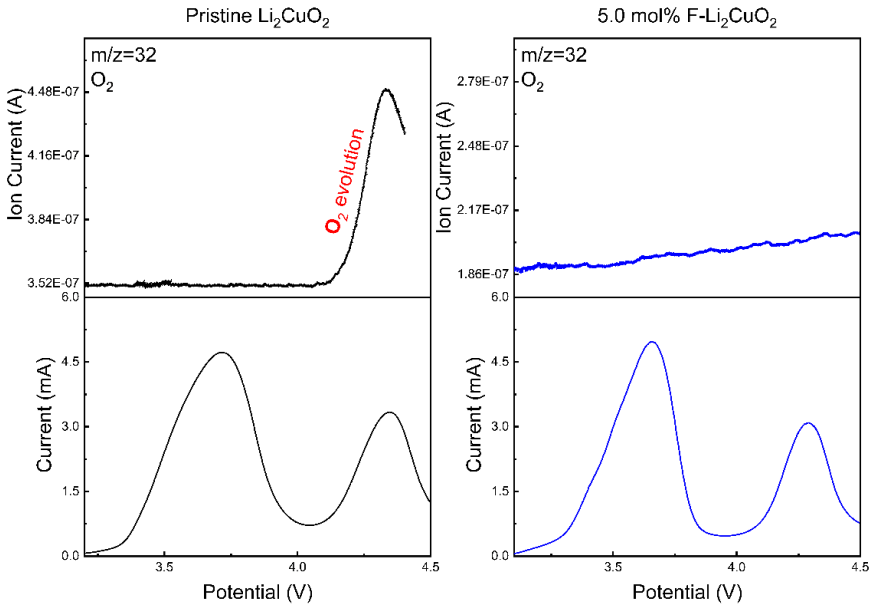

Fig. 6. Linear step voltammograms and Oxygen (m/z = 32) ion current of Li^0|1 M $LiPF_6$|Active material: carbon black: PVDF (75:15:10 wt%) cells. Adapted with permission from Ref.[15]. Copyright 2020 American Chemical Society.

Although doping is a suitable strategy, the solubility of an ion within a crystalline structural is crucial, exceeding the solubility limit can lead to the formation of other phases or impurities that may either enhance or limit the capacity of an active material. Several publications report the effect of additional ions within the structure; however, the presence of impurities or secondary phases make it impossible to make a fair comparison.

To analyze the effect of secondary phases formation, Martínez-Cruz et al. [28] synthesized the phase $Li_2Cu_{0.5}Ni_{0.5}O_2$/$LiNi_{0.5}Cu_{0.5}O_2$ (orthorhombic/rhombohedral phase, respectively) using the solid-state method under different atmospheres: N_2, air, or O_2. The materials synthesized in an oxygen atmosphere exhibited superior electrochemical performance due to a higher weight percentage of the $LiNi_{0.5}Cu_{0.5}O_2$ phase compared to the material obtained under other atmospheres. In situ XRD demonstrated that the rhombohedral phase enhances charge retention and structural reversibility (Fig. 7). During charging of LiNiCu-O_2, signals from both rhombohedral and orthorhombic phases are observed. However, at the 3.4 V plateau, reflections from the orthorhombic phase decrease in intensity, while those from the rhombohedral phase remain stable, indicating that the latter does not participate in the electrochemical process. In the second plateau, at 3.7 V, the reflections from the rhombohedral phase undergo directional changes, suggesting alterations in the crystalline structure during lithium ion deintercalation. At 4.2 V, with increased oxidation, signals from the rhombohedral phase continue to shift in the same direction as in the previous plateau. During discharge, reflections from the rhombohedral phase return to their original values, while those from the orthorhombic phase significantly lose intensity, indicating a collapse in the crystal lattice like that observed in Li_2CuO_2. Changes in reflections from the rhombohedral phase during charging suggest a decrease in the parameter "a" and an increase in the parameter "c", which are reversed during discharge, indicating structural reversibility likely related to the presence of Cu^{3+} in the $LiNiO_2$ structure.

To better understand the effect of copper on $LiNiO_2$ (LNO), in situ XRD analysis was conducted on both LNO and Cu-LNO samples (Fig. 8**(a)**). This analysis allowed observation of the changes occurring at higher potentials (phase transitions), facilitating the correlation between capacity retention and structural stability. The in situ XRD experiments indicate that the main degradation mechanism is related to the increased fraction of the formed phase (Fig. 8**(b)**) and changes in interlayer distances (Fig. 8**(c)**). These characteristics confirm a positive effect of copper inclusion.

J. Mex. Chem. Soc. **2024**, *68*(4)
Special Issue

ISSN-e 2594-0317

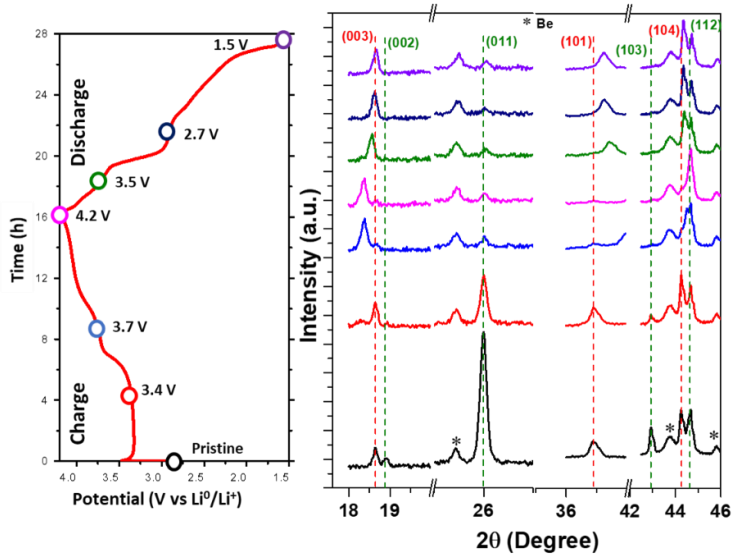

Fig. 7. In situ XRD patterns of $Li_2Cu_{0.5}Ni_{0.5}O_2$/$LiNi_{0.5}Cu_{0.5}O_2$ in lithium half-cell cycled between 1.5 – 4.2 V at C/15 rate. The green and red vertical dashed lines in the direction patterns indicate peaks related to the orthorhombic and rhombohedral phases, respectively. Figure reproduced from [28] with the author's permission.

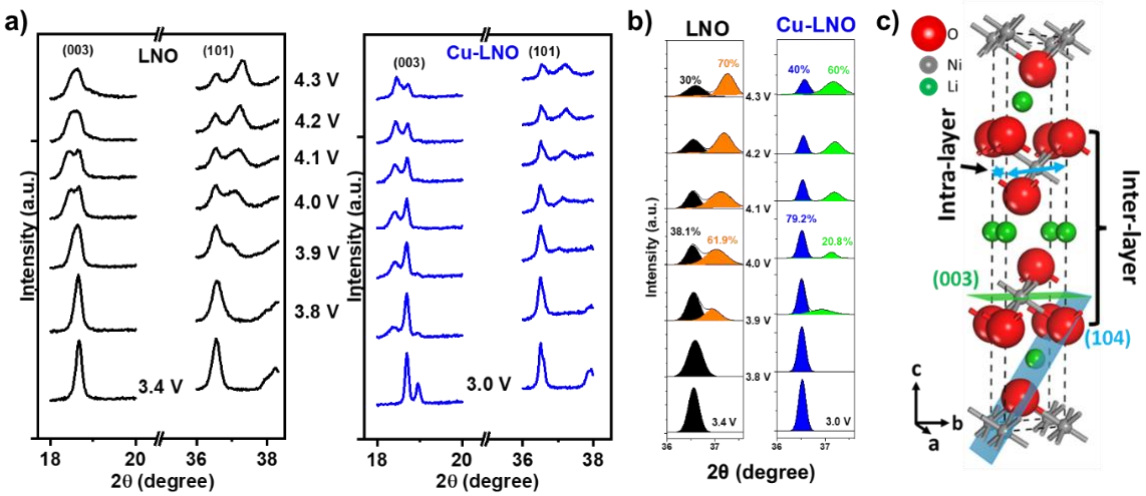

Fig. 8. (a) In situ XRD patterns of LNO and Cu-LNO in lithium half-cell cycled between 3.0 – 4.3 V at C/15 rate. **(b)** The relative fraction of phase transitions was obtained through the deconvolution of the (101) plane reflection in the in situ XRD pattern during charging. The black and blue areas correspond to the fractions of the initial phases, while the orange and green areas correspond to the phases formed during charging. **(c)** Schematic representation of the LNO unit cell. Figure reproduced from [28] with the author's permission.

The results obtained are consistent with other modifications previously performed on $LiNiO_2$, in which the substitution of other transition metal ions in the Ni positions improve the reversibility of H2 to H3 phases at high potentials, providing greater structural stability that is reflected in capacity retention [29–32]. Therefore, the Cu-LNO phase proves to be attractive as a cathode material for LIBs, although a phase mixture is obtained, the results indicate an overall improvement over the pure phase.

J. Mex. Chem. Soc. **2024**, *68*(4)
Special Issue

ISSN-e 2594-0317

Li_2CuO_2 dual doping: Anionic and cationic agents

Lastly, we present for the first time our most recent efforts to modify Li_2CuO_2 using a dual-doping strategy. These new results use both cationic and anionic dopants, specifically using manganese and fluorine. This is done to inhibit oxygen from participating in the redox processes during the initial extraction of Li, thereby preventing the formation of O_2. The F^- ions occupy the sites where O resides in the Li_2CuO_2 lattice, and doping with Mn also causes modifications in the cell parameters that provide structural stability. The synthesized material, containing up to 5.0 % dopants is stable and isostructural to Li_2CuO_2 (Fig. 9).

Galvanostatic cycling was carried out at C/10 using Li_2CuO_2 cathode electrodes doped with Mn and F prepared under inert conditions. The materials that have been dual-doped display a second plateau, which is associated with oxygen evolution around 4.1V. However, it's important to note that the materials with 2.5 % and 3.5 % doping show a less pronounced plateau compared to the other materials. It can be inferred that the amount of oxygen remaining within the material's network is higher in these cases, compared to the others where more O_2 is formed. During the discharge process, Cu^{+1} is formed in all materials, contributing to material degradation. By cycle 10, the only material that shows improvement over the pristine material is the one with 3.5 % MnF_2, as evidenced by the charge retention in Fig. 10.

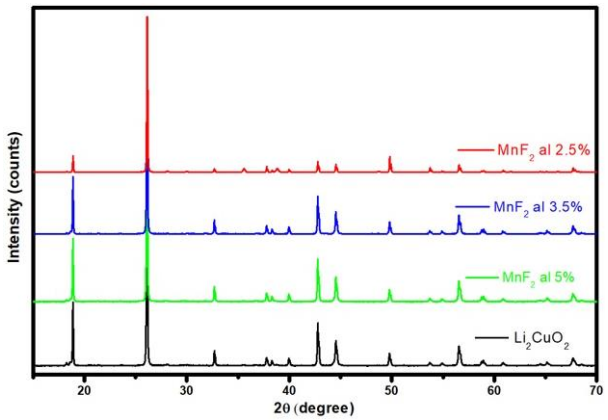

Fig. 9. XRD of dual anionic and cation doping Li_2CuO_2 with MnF_2 at 2.5 %, 3.5 % and 5.0 %.

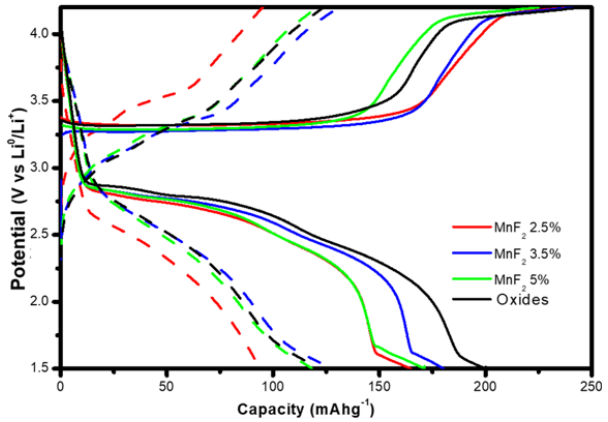

Fig. 10. Charge/discharge diagram of Li_2CuO_2 doped with MnF_2 at 2.5 %, 3.5 %, and 5.0 % of Li^0|1 M $LiPF_6$|Active material: carbon black: PVDF (75:15:10 wt%) cells, cycled at C/10 at 25°C. The solid line represents the first cycle, and the dashed line represents cycle 10.

J. Mex. Chem. Soc. **2024**, *68*(4)
Special Issue

ISSN-e 2594-0317

Finally, Table 1 summarizes the various modifications and effects on the structure and electrochemical properties of Li_2CuO_2, based on the results discussed in this work.

Table 1. Summary of widely investigated dopants and their effect on Li_2CuO_2.

Dopants	Description	Key results	References
Undoped	Pure Li_2CuO_2 phase.	Baseline capacity and performance, prone to oxygen evolution and structural instability.	[16]
Ni	Incorporation of 50 % Ni to form secondary phase.	Increase in capacity and introduction of new redox processes.	[17]
Ni	5 mol % of Ni^{2+} to form solid solutions.	Higher initial capacity but generation of new irreversible phase.	[12]
Mn	Doping with 5 mol % Mn^{4+}.	Improvement in structural stability, reduction in O_2 evolution.	[12]
Fe	Limited solubility of Fe^{3+} at 5 mol%.	Increase in specific capacity, but higher O_2 evolution.	[12]
F	Anionic doping, replacement of O^{2-} with F^-.	Improvement in coulombic efficiency, inhibition of oxygen evolution.	[15]
Mn and Co	Dual doping with Mn^{4+} and Co^{2+}.	Marginal increase in reversible capacity and capacity retention.	[20]
Mn and Ni	Dual doping with Mn^{4+} and Ni^{2+}.	No significant increase in capacity compared to the pure material.	[20]
Mn and F	Anionic (F^-) and cationic (Mn^{4+}) doping.	No significant improvement compared to individual doping.	Reported herein
Ni	Phase control, synthesis under different atmosphere.	Improved electrochemical performance, higher $LiNi_{0.5}Cu_{0.5}O_2$ phase as a result of synthesis in O2 atmosphere.	[28]

Conclusions

Numerous strategies have been explored to modify the electrochemical properties of Li_2CuO_2, primarily aiming to enhance its electrochemical and structural reversibility. Although these modifications have not yet yielded a reversible capacity that renders this material practical, they have increased the specific capacity by introducing redox active centers. Moreover, comprehensive studies of this material have shown that while inactive centers bolster structural stability, they decrease capacity. Anion doping has proven effective in mitigating oxygen evolution at higher potentials. However, despite efforts in dual doping and element combinations, none have resulted in significant improvements compared to individual doping.

J. Mex. Chem. Soc. **2024**, *68*(4)
Special Issue

ISSN-e 2594-0317

Therefore, we propose that future advancements in Li_2CuO_2 could involve applying successful techniques and knowledge from other cathode chemistries. For example, the impact of crystallinity (single crystal vs. polycrystalline) and faceting on various cathodes has been well-documented, demonstrating that cycling performance and oxygen loss inhibition can be achieved by controlling the crystallography of the active material [33,34]. Although single crystal Li_2CuO_2 has been successfully synthesized in characterization reports, the electrochemical performance of single crystal Li_2CuO_2 electrodes remains unexplored [35,36]. Investigating this could lead to a deeper understanding of Li_2CuO_2 and potential performance improvements.

Furthermore, it is widely recognized that the electrode-electrolyte interface plays a critical role in achieving long, stable cycling, especially since electrode redox reactions and degradation originate at this interface [37,38]. Therefore, future studies should prioritize stabilizing the electrolyte – Li_2CuO_2 interface. Protective coatings such as $LiNbO_3$, for instance, have been shown to enhance rate capability and improve capacity retention [39–41].

In conclusion, there are still abundant opportunities to apply our learnings to further enhance Li_2CuO_2. With ongoing research and development, we remain hopeful that Li_2CuO_2 will eventually emerge as a viable Li-ion cathode material for Li-ion batteries.

Acknowledgements

A. de J. Martinez-Maldonado, B. A. García-Carrillo and E.L. Jimenez-Cabañas are grateful for the scholarship granted to them by CONAHCYT to pursue their graduate studies. The authors would like to thank Federico Gonzalez for XRD measurements and extend their most sincere gratitude to the collaborators and laboratories of the Universidad Autónoma Metropolitana (Unidad Iztapalapa), especially to Ignacio González Martínez, for his valuable contribution during the development of this work. This work was performed as part of the consortium stablished by the National Laboratory CONAHCYT BIL-DEMo. This work was possible thanks to CONAHCYT support grants FORDECYT-PRONACES/1560340/2020, Apoyos LNC 2023-123, CF-2023-G-918 and CF-2023-G-1266.

References

1. Jäger-Waldau A. *EPJ Photovoltaics*, **2022**, 13. DOI: https://doi.org/10.1051/epjpv/2022010.
2. Summerfield-Ryan O., Park S., *Ecological Economics*, **2023**, 210, 107841. DOI: https://doi.org/10.1016/j.ecolecon.2023.107841.
3. Perez M., Perez R., *Solar Energy Advances*, **2022**, 2, 100014. DOI: https://doi.org/10.1016/j.seja.2022.100014.
4. Vivoda V., Bazilian M.D., Khadim A., Ralph N., Krame G., *Energy Res Soc Sci*, **2024**, 108, 103393. DOI: https://doi.org/10.1016/j.erss.2023.103393.
5. Hoppe R., Rieck H, *Zeitschrift für anorganische und allgemeine Chemie,* **1970**, 379, 2, 157-164. DOI: https://doi.org/10.1002/zaac.19703790206.
6. Hoffmann R., Hoppe R., Schäfer W., *Zeitschrift für anorganische und allgemeine Chemie,* **1989**, 578, 1, 18-26. DOI: https://doi.org/10.1002/zaac.19895780103.
7. Sapiña F., Rodríguez-Carvajal J., Sanchis M.J., Ibáñez R., Beltrán A., Beltrán D., *Solid State Commun*, **1990**, 74, 779–784. DOI: https://doi.org/10.1016/0038-1098(90)90934-4.
8. Prakash A.S., Larcher D., Morcrette M., Hegde M.S., Leriche J., **2005**, 74, 4406–4415. DOI: https://doi.org/10.1021/cm0508266.
9. Ruther R.E., Samuthira Pandian A., Yan P., Weker J.N., Wang C., Nanda J., *Chemistry of Materials*, **2017**, 29, 2997–3005. DOI: https://doi.org/10.1021/acs.chemmater.6b05442.
10. Ruther R.E., Zhou H., Dhital C., Saravanan K., Kercher A.K., Chen G., *et al.*, *Chemistry of Materials*, **2015**, 27, 6746–6754. DOI: https://doi.org/10.1021/acs.chemmater.5b02843.

J. Mex. Chem. Soc. **2024**, *68*(4)
Special Issue

ISSN-e 2594-0317

11. Xu J., Renfrew S., Marcus M.A., Sun M., McCloskey B.D., Tong W., *Journal of Physical Chemistry C*, **2017**, 121, 11100–11107. DOI: https://doi.org/10.1021/acs.jpcc.7b01799.
12. Martínez-Cruz M.A., Yañez-Aulestia A., Ramos-Sánchez G., Oliver-Tolentino M., Vera M., Pfeiffer H., *et al.*, *Dalton Transactions*, **2020**, 49, 4549–4558. DOI: https://doi.org/10.1039/D0DT00273A.
13. Arachi Y., Ide T., Nakagawa T., Nakata Y., *ECS Trans*, **2012**, 50, 143–151. DOI: https://doi.org/10.1149/05024.0143ecst.
14. Perea-Ramírez L.I., Guevara-García A., Galván M., *J Mol Model*, **2018**, 24, 227. DOI: https://doi.org/10.1007/s00894-018-3754-0.
15. Juarez-Yescas C., Oliver-Tolentino M., Ramos-Sánchez G., Vera-Ramirez M.A., Olmedo-González J., Ochoa-Calle A., *et al.*, *ACS Appl Energy Mater*, **2020**, 3, 2771–2780. DOI: https://doi.org/10.1021/acsaem.9b02429.
16. Ramos-Sanchez G., Romero-Ibarra I.C., Vazquez-Arenas J., Tapia C., Aguilar-Eseiza N., Gonzalez I., *Solid State Ion*, **2017**, 303, 89–96. DOI: https://doi.org/10.1016/j.ssi.2017.02.018.
17. Aguilar-Eseiza N., Ramos-Sánchez G., González F., González I., *Electrochem Commun*, **2018**, 96, 32–36. DOI: https://doi.org/10.1016/j.elecom.2018.09.002.
18. Shannon R.D., *Acta Crystallographica Section A*, **1976**, 32, 768–771. DOI: https://doi.org/10.1107/S0567739476001551.
19. Mizuno Y., Tohyama T., Maekawa S., *Phys Rev B Condens Matter Mater Phys*, **1999**, 60, 6230–6233. DOI: https://doi.org/10.1103/PhysRevB.60.6230.
20. Garcia Carrillo B.A., Estudio de cuprato de litio modificado con iones de metales de transición como cátodo alternativo para baterías de ion litio, Universidad Autónoma Metropolitana, **2023**
21. Weng Y., Zhang H., *Ionics (Kiel)*, **2024**, 30, 1885–1895. DOI: https://doi.org/10.1007/s11581-023-05366-4.
22. He Z., Zhang M., Zhou K., Cheng Y., Luo M., Su Y., *et al.*, *ACS Appl Energy Mater*, **2023**, 6, 3422–3431. DOI: https://doi.org/10.1021/acsaem.2c04133.
23. Ahn H., Choi J., Kim M., Kyu Kang S., Jang D., Maeng J., *et al.*, *Chemistry of Materials*, **2024**, 36, 9, 4379-4392. DOI: https://doi.org/10.1021/acs.chemmater.3c03307.
24. Kong F., Liang C., Longo R.C., Yeon D.H., Zheng Y., Park J.H., *et al.*, *Chemistry of Materials*, **2016**, 28, 6942–6952. DOI: https://doi.org/10.1021/acs.chemmater.6b02627.
25. Kim H., Kim S.B., Park D.H., Park K.W., *Energies (Basel)*, **2020**, 13, 4808-4817. DOI: https://doi.org/10.3390/en13184808.
26. Lin Y., Zhong K., Zheng J., Liang M., Xu G., Feng Q., *et al.*, *ACS Appl Energy Mater*, **2021**, 4, 9848–9857. DOI: https://doi.org/10.1021/acsaem.1c01883.
27. Dai K., Wu J., Zhuo Z., Li Q., Sallis S., Mao J., *et al.*, *Joule*, **2019**, 3, 518–541. DOI: https://doi.org/10.1016/j.joule.2018.11.014.
28. Martínez-Cruz M.A., Ramos-Sánchez G., Oliver-Tolentino M., Pfeiffer H., González I., *J Alloys Compd*, **2022**, 923, 166328. DOI: https://doi.org/10.1016/j.jallcom.2022.166328.
29. Zhang Y., Li H., Liu J., Liu J., Ma H., Cheng F., *Journal of Energy Chemistry*, **2021**, 63, 312-319. DOI: https://doi.org/10.1016/j.jechem.2021.07.029.
30. Ryu H.H., Park G.T., Yoon C.S., Sun Y.K., *J Mater Chem A Mater*, **2019**, 7, 18580–18588. DOI: https://doi.org/10.1039/C9TA06402H.
31. Hao Q., Du F., Xu T., Zhou Q., Cao H., Fan Z., *et al.*, *Journal of Electroanalytical Chemistry*, **2022**, 907, 116034. DOI: https://doi.org/10.1016/j.jelechem.2022.116034.
32. Goonetilleke D., Mazilkin A., Weber D., Ma Y., Fauth F., Janek J., *et al.*, *J Mater Chem A Mater*, **2022**, 10, 7841–7855. DOI: https://doi.org/10.1039/D1TA10568J.
33. Zhang F., Zhou X., Fu X., Wang C., Wang B., Liang W., *et al.*, *Mater Today Energy*, **2021**, 22, 100873. DOI: https://doi.org/10.1016/j.mtener.2021.100873.
34. Li J., Cameron A.R., Li H., Glazier S., Xiong D., Chatzidakis M., *et al.*, *J Electrochem Soc*, **2017**, 164, A1534–A1544. DOI: https://doi.org/10.1149/2.0991707jes.
35. Balodhi A., Kim M.G., *Crystals (Basel)*, **2024**, 14, 288. DOI: https://doi.org/10.3390/cryst14030288.

J. Mex. Chem. Soc. **2024**, *68*(4)
Special Issue

ISSN-e 2594-0317

36. Kawamata S., Okuda K., Kindo K., *J Magn Magn Mater*, **2004**, 272–276, 939–940. DOI: https://doi.org/10.1016/j.jmmm.2003.12.579.
37. Hausbrand R., Cherkashinin G., Ehrenberg H., Gröting M., Albe K., Hess C., *et al.*, *Materials Science and Engineering: B*, **2015**, 192, 3–25. DOI: https://doi.org/10.1016/j.mseb.2014.11.014.
38. Minato T., Abe T., *Prog Surf Sci*, **2017**, 92, 240–280. DOI: https://doi.org/10.1016/j.progsurf.2017.10.001.
39. Xin F., Zhou H., Chen X., Zuba M., Chernova N., Zhou G., *et al.*, *ACS Appl Mater Interfaces*, **2019**, 11, 34889–34894. DOI: https://doi.org/10.1021/acsami.9b09696.
40. Takada K., Ohta N., Zhang L., Fukuda K., Sakaguchi I., Ma R., *et al.*, *Solid State Ion*, **2008**, 179, 1333–1337. DOI: https://doi.org/10.1016/j.ssi.2008.02.017.
41. Li X., Jin L., Song D., Zhang H., Shi X., Wang Z., *et al.*, *Journal of Energy Chemistry*, **2020**, 40, 39–45. DOI: https://doi.org/10.1016/j.jechem.2019.02.006.